Destruction cross sections for fast hydrogen molecules incident on helium, neon, and argon

N.V. de Castro Faria, I. Borges, Jr., L.F.S. Coelho, and Ginette Jalbert
Instituto de Física, Universidade Federal do Rio de Janeiro, Caixa Postal 68 528, Rio de Janeiro, 21 945, Rio de Janeiro, Brazil
(Received 31 May 1994)

We measured the destruction cross sections of fast H_2 molecules ($3.0 \leq v \leq 7.0$ a.u.) in helium, neon, and argon targets. We also measured, complementing previously published data, the H_2^+ destruction cross sections in neon for $3.0 \leq v \leq 7.0$ a.u. and in helium and argon for $v = 3.0$ a.u. The H_2 beam was obtained from fast H_3^+ molecules dissociated in an auxiliary target. These H_2 and H_2^+ destruction cross sections were compared with the previous ones for H_2^+ and H_3^+ ions and also with the H electron-loss cross section, and a simple description is able to explain quantitatively the observed trends for these four sets of experiments, giving also information about the main destruction channels for the H_2 and H_2^+ molecules.

PACS number(s): 34.90.+q

I. INTRODUCTION

High-energy molecular fragmentation is a basic problem, particularly for the simplest molecules H_2, H_2^+, and H_3^+, as it yields information both on the molecular structure and on the collision itself. However, although the literature presents experimental results of collision processes at intermediate and high energies involving H_2^+ ions [1–6], and also for H_3^+ ions [6–12], few of these works deal with a wide range of energies and even less make a systematic choice of targets. In particular, the lack of systematic data for fast H_2 molecules colliding with noble gas targets prevents comparing H_2^+ and H_3^+ data at the same velocities and colliding with the same targets, such comparison being needed in order to build models for molecular dissociation [13] and hydrogen cluster fragmentation.

We have systematically studied collisions of fast H_3^+ and H_2^+ molecules with He, Ne, Ar, and, eventually, Xe gas targets, these ions being produced in a radio frequency ion source and subsequently accelerated to velocities going from 3.0 to 7.0 a.u. Up to now the H_3^+ measurements include the total destruction cross section [7], the center-of-mass distribution of H^- and H^+ ions [8], and the production of H^- ions [9] and neutral fragments [10]. The study of fast H_2^+ collisions started by measuring the total destruction cross sections in helium and argon ($4.0 \leq v \leq 7.0$ a.u.) [5]. Additional H_2^+ destruction results are given in the present paper for a neon target and $3.0 \leq v \leq 7.0$ a.u. and for helium and argon targets at $v = 3.0$ a.u.

It is also possible to obtain beams of fast H atoms and H_2 molecules, through the fragmentation of H_3^+ molecules followed by the removal of the charged fragments. In this paper we present the first, as far as the authors are aware, measured values of the destruction cross sections for fast H_2 molecules. This process has only been studied by electron and photon impact (a recent review is presented in Ref. [14]). In this paper we also discuss the H_2 and the H_2^+ data in terms of a simple model, which describes well the data for the several targets (He, Ne, and Ar) and the different projectiles (H_2, H_2^+, and H_3^+).

II. EXPERIMENTAL ARRANGEMENT AND METHODS

A scheme of the experimental setup is shown in Fig. 1 (a previous and similar arrangement has already been described [7]). The H_3^+ ions were produced by a radio frequency ion source, accelerated by the PUC-Rio 4 MV Van de Graaff accelerator and momentum selected by a 90° magnet. By closing the vacuum pump located near this magnet, a preliminary 1 m long target was formed by the residual gases, going from the magnet exit to stabilizing slits. This target breaks some of the H_3^+ molecules into neutral and charged fragments, the latter being removed by a permanent magnet placed just after the stabilizing slits. Neutral fragments eventually ionized by the residual gas before reaching the target were removed from the beam by another permanent magnet, 2 m apart, located just before the slit system at the entrance of the chamber containing the gas cell. This slit system limited the beam intensity to values as low as a thousand particles per second, thus allowing the use of a surface barrier detector for the transmitted neutral particles. An arrangement already employed in the previous [7] H_3^+ destruction measurement allowed monitoring of nonconstant beam currents: an auxiliary surface barrier detector facing a rotating gold target placed on a beam chopper and counting the Rutherford scattered (90°) particles. This arrangement was not employed for the present experiments as improved accelerator conditions led to constant intensity beams.

The differentially pumped target system was composed of a 10 cm long gas cell, with the diameters of the entrance and exit openings being, respectively, equal to 0.5

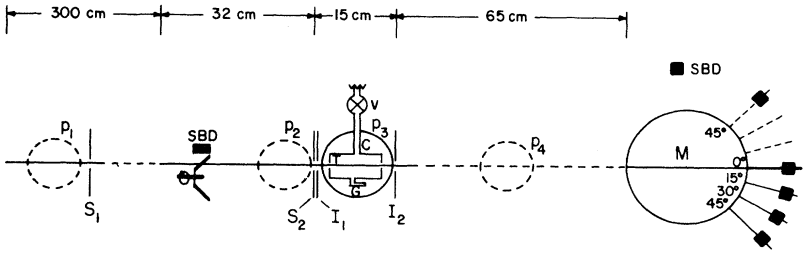

FIG. 1. Scheme of the experimental setup (the drawing is not to scale). The symbols should read: P_1, P_2, and P_3 are diffusion vacuum pumps; I_1 and I_2 are vacuum impedances; S_1 and S_2 are collimation slits; V is a gas valve; T is the target; G is a thermocouple pressure gauge; C is the chamber containing the target; SBD is a surface barrier detector; and M is the switching magnet.

and 2.0 mm, placed in a vacuum chamber pumped by a 4 in. diffusion pump. The cell pressure was measured employing a thermocouple device, calibrated, for each gas, against a Baratron capacitive manometer. The uncertainty arising from this calibration procedure was smaller than 1%. Before entering the chamber the beam was collimated by a set of staggered crossed pairs of micrometric sliding slits, defining beam dimensions always smaller than 0.1×0.1 mm^2 and reducing its intensity in order to allow the use of a surface barrier detector. The chamber was isolated from the beamline by entrance and exit vacuum impedances, with diameters of 0.5 and 5.0 mm respectively and indicated in Fig. 1, leading to chamber pressures outside the gas cell that were a factor of a thousand lower than the ones inside. Low beamline pressures were ensured by the small size of the entrance impedance opening, reducing the gas flow from the chamber, and by the employment of one 2 in. and one 4 in. diffusion pump, placed just outside the chamber impedances. As the fragments acquired transversal momentum from internal molecular energy, the lighter H atoms suffered a larger angular deflection than the heavier H_2 molecule; thereby this entrance aperture, together with the micrometric slits, reduces preferentially the number of H atoms, single or in pairs, reaching the gas target. A similar arrangement using an iris aperture was employed by Nir and co-workers [1] to study the H_2^+ fragmentation but with the different purpose of ensuring the full collection of the fragments.

The scattering chamber was followed by a magnetic switch with seven exits, one at 0° and three on each side at the angles ±15°, ±30°, and ±45°, where different fragments could be simultaneously measured, as was done in Refs. [5,7–10]. In the present H_2 attenuation measurements only the 0° exit was needed.

Besides the H_3^+ fragmentation in the auxiliary target, neutral particles reaching the target could also be generated by processes occurring between the two auxiliary magnets. One such process, negligible at these velocities, was electron capture by H^+ and H_2^+ ions, associated with small momentum transfers and therefore leading to neutral particles still remaining in the beam. Another process was H_2 fragmentation into H-H pairs. If it occurred near the target cell entrance the fragments would reach the target but it has been shown [14] that this H_2 dissociation channel was totally negligible for electrons with similar velocities. The residual gas pressure between the two magnets was low, particularly near the cell entrance where a diffusion pump ensured 10^{-6} Torr, further reducing contributions from this region. As the H-H pairs came from a region at least 2 m away from the target cell and their angular spread, owing to their lighter mass, was larger than the one for H_2 molecules, these pairs were expected to be strongly discriminated by the collimators placed before the gas cell.

The H_2 transmitted molecules were measured by a large (25 mm diam) surface barrier detector. For different target pressures (about ten values, the first and the last ones being the background) the number of transmitted particles was measured at fixed time intervals. The H_2 total destruction cross section was then obtained by fitting the transmitted "double-mass events" as the sum of the transmitted molecules and pairs of atoms:

$$N_{\mathrm{II}}(\pi) = N^0_{\mathrm{H_2}} e^{-\sigma_D^{\mathrm{H_2}}\pi} + N^0_{\mathrm{HH}} e^{-2\sigma_{01}\pi},$$

where $N_{\mathrm{II}}(\pi)$ is the measured number of "double-mass events" (H_2 and H-H), $N^0_{\mathrm{H_2}}$ and N^0_{HH} are the respective numbers of H_2 molecules and H-H pairs incident upon the gas target, π is the product of the target density and length, $\sigma_D^{\mathrm{H_2}}$ is the destruction cross section for the H_2 molecules, and σ_{01} is the loss cross section for H atoms. In the above expression processes such as $H_2 \rightarrow H_2^+ \rightarrow H_2$ and $H_2 \rightarrow$H-H were neglected, the reasons being the same as the ones employed in the residual gas processes: at these high velocities electron capture is negligible and H_2 fragmentation is expected to proceed through single and double ionization.

The χ^2 curve yields a value for $\sigma_D^{\mathrm{H_2}}$ but is very flat for variations of the N^0_{HH} and $N^0_{\mathrm{H_2}}$ parameters, with the similarity of the $\sigma_D^{\mathrm{H_2}}$ and $2\sigma_{01}$ values precluding the extraction of the parameters' exact values. Even so, these two parameters may be extracted with large uncertainties and N^0_{HH} seems to be much smaller than $N^0_{\mathrm{H_2}}$, reflecting more the strict collimation than the collision yield for the respective H_3^+ fragmentation channels.

In order to account for possible beam fluctuations, at least four experimental runs were done for each target and energy value, leading to independently obtained cross section values. The final result, for a given target and a given energy, was the arithmetic average of these cross section values, their standard deviation accounting for statistical, fitting procedure, and beam instability errors.

The present results of the H_2^+ attenuation were measured with the same gas target, pumping system, and slit system above described, with two obvious differences: the 90° magnet vacuum pump was left open and no permanent magnets were used. The transmitted H_2^+ ions were detected on the ±45° switch magnet exit. A surface barrier detector was used for small beam currents, otherwise

a Faraday cup was employed. The experimental cross sections were obtained by fitting a single-exponential function to the normalized beam attenuation.

III. RESULTS AND DISCUSSION

The H_2 destruction cross sections for helium, neon, and argon targets measured in this work are presented in Table I (the experimental conditions did not allow measuring the cross sections for $v = 6$ in Ar and $v = 7$ in Ne). Table II contains the H_2^+ destruction cross sections for the same gases and velocity range, and includes, for completeness, our previous results [5]. A semiempirical formula for atomic ionization [15], already applied to the H_3^+ destruction problem after some simplifications [7], described well the cross section velocity dependence as $1/\sigma = a + bv^2$. This fitting procedure for the H_2 and H_2^+ destruction cross sections, here shown in Figs. 2 and 3, respectively, was employed in order to smooth experimental fluctuations, for better data comparison and interpretation, with the values so obtained also being presented in parentheses in Tables I and II.

In order to interpret these data one may first look at the projectile dependence. It is then useful to compare, for the same targets and velocities, the H_2 and H_2^+ data with the H and H_3^+ destruction cross sections. One may consider the collision as a *free* projectile electron moving with the projectile velocity and colliding with a *static* noble gas target and a simple expression for the destruction of molecular projectiles, detailed below, then allows this comparison to be made [13]. Secondly, one may look at the target dependence of these two collision processes.

Salpeter [13] gives an expression where the molecular destruction cross sections are inversely proportional to the dissociation energy I. This expression is based on a model for atomic ionization proposed by Bohr [16], where the energy I is defined as the one needed to excite the molecule, placed at its equilibrium internuclear distance, from its electronic and vibrational ground state to the first dissociative electronic state. The basic assumption of this model is the free movement of the projectile components, leading to destruction cross sections directly proportional to the number of projectile electrons, n. We then defined $\sigma I/n$ as a normalized cross section value S, where the σ values employed were the smoothed ones coming from the interpolation procedure. The results for each projectile are presented in Tables III, IV, and V divided by S_H, the I values employed being [18,7,13]

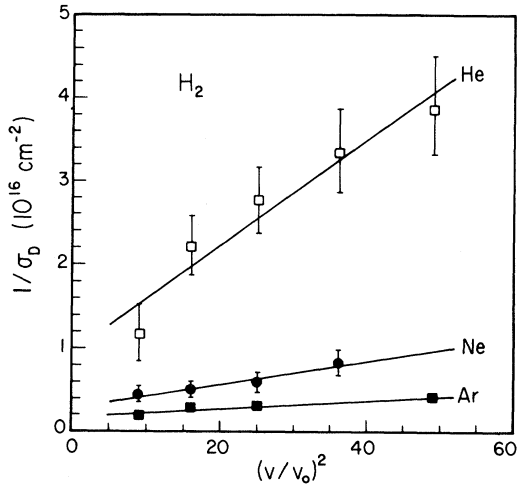

FIG. 2. Experimental H_2 destruction cross sections for He, Ne, and Ar targets, plotted as σ^{-1} versus v^2 and fitted to straight lines, as justified on a semiempirical basis (the error bar is not shown when the standard deviation of a data point is smaller than the point symbol size).

16.3 eV for H_2 and 13.6 eV for H corresponding to the respective ionization energies, 12.5 eV for H_2^+ transition to the dissociative state $2p\sigma_u$ and 15.4 eV for H_3^+ corresponding to the dissociative state $^3E'$. Concerning the H_2 destruction by fast electrons, it is already known [14] to proceed through ionization and not through the excited triplet state of H_2, $b\,^3\Sigma_u^+$ (its first dissociative state). To test this hypothesis for H_2 destruction by noble gases we tried tentatively two I values, namely, 16.3 eV as mentioned above and 10.0 eV, corresponding to the first dissociative state. The former seems to be the dominant process for the H_2 destruction induced by collisions with noble gases, as this leads to normalized values agreeing much better with the ones for the other projectiles.

Tables III, IV, and V show, respectively for He, Ne, and Ar targets, the normalized cross section values for H_2^+, H_2, and H_3^+ divided by S_H. Several interesting conclusions may be drawn from these tables. First of all, $S_{\text{projectile}}/S_H$ is roughly equal to unity, the overall average of the 45 ratios $S_{\text{projectile}}/S_H$ being equal to 0.97 and its standard deviation 0.20. The small spread of these data and their closeness to unity are surprising, as the data include, for velocities ranging from 3.0 to 7.0 a.u., three different molecular projectiles and three dif-

TABLE I. H_2 destruction cross sections for He, Ne, and Ar targets (measured values, followed by the interpolated values in parentheses).

Velocity (a.u.)	$\sigma_D^{H_2}$ (10^{-16} cm^2)		
	He	Ne	Ar
3.0	0.85±0.09(0.80)	2.2±0.1(2.3)	5.0±0.5(4.8)
4.0	0.45±0.07(0.56)	1.8±0.3(1.9)	3.5±0.5(4.0)
5.0	0.36±0.04(0.41)	1.6±0.3(1.5)	3.2±0.3(3.4)
6.0	0.30±0.03(0.30)	1.1±0.2(1.2)	not measured (2.8)
7.0	0.26±0.03(0.23)	not measured (1.0)	2.5±0.3(2.4)

TABLE II. H_2^+ destruction cross sections for He, Ne, and Ar targets (measured values, followed by the interpolated values in parentheses).

Velocity (a.u.)	$\sigma_D^{H_2^+}$ (10^{-16} cm^2)		
	He	Ne	Ar
3.0	0.64±0.04(0.61)	2.0±0.1(2.0)	3.8±0.1(3.7)
4.0	0.44±0.09(0.47)	1.6±0.1(1.6)	3.2±0.1(3.1)
5.0	0.39±0.05(0.36)	1.2±0.1(1.2)	2.3±0.2(2.6)
6.0	0.27±0.03(0.28)	0.94±0.05(0.97)	2.3±0.3(2.1)
7.0	0.22±0.04(0.22)	0.80±0.10(0.78)	1.8±0.1(1.8)

ferent noble gas targets. The simple Salpeter approach accounts then for the main characteristics of the molecular projectiles, even neglecting the higher dissociative states and considering the molecular ions produced in the rf ion source to be in the lowest vibrational state (the vibrational excitation may lead to an internal energy around 1 eV, for a typical rf ion source [7]).

A qualitative view of these data, for a given target, shows that the normalized cross sections present essentially the same velocity dependence and, if in addition one fixes the velocity, the data present a very small projectile dependence, both results to be expected from the Salpeter approach. A more stringent test will then be the analysis of the target, the projectile, and the velocity dependences of these ratios and to see whether these individual averages significantly differ from unity. For each target, the result of a statistical analysis of data for the three different projectiles and the five different velocities was 1.14±0.27 for He, 0.86±0.08 for Ne, and 0.92±0.07 for Ar. The three cases present near-unity averages, with the Ne and the Ar data having standard deviations of less than 10%. In the He case a velocity dependence is present and leads to a standard deviation around 25%. When looking, in a similar way, at the projectile and the velocity dependences of these ratios, we again find near-unity averages. The averages and standard deviations for the several projectiles are 1.08±0.22 for H_2^+, 0.86±0.11 for H_2, and 0.96±0.18 for H_3^+, the presence of the He data leading to larger values of the standard deviations. The velocity dependence of the data, obtained by averaging data for the three projectiles and the three targets, reflects again the clear velocity dependence of the He case, attenuated, however, by the smaller dependences for Ne and Ar: 0.85±0.10 for $v = 3$, 0.93 ± 0.10 for $v = 4$, 0.99 ± 0.17 for $v = 5$, 1.02 ± 0.23 for $v = 6$, and 1.05 ± 0.27 for $v = 7$. The presence of this velocity dependence for the He target may be related to its ionization potential being the largest for the three targets, thereby increasing the minimum velocity for a free collision model (FCM) description to be valid.

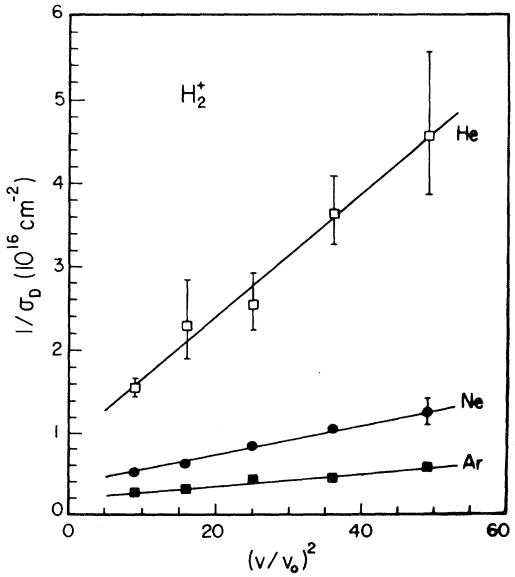

FIG. 3. Experimental H_2^+ destruction cross sections for He, Ne, and Ar targets, plotted as σ^{-1} versus v^2 and fitted to straight lines, as justified on a semiempirical basis. (The error bar is not shown when the standard deviation of a data point is smaller than the point symbol size.)

The destruction cross sections for fast molecular projectiles are expected to grow with the size of the atomic target [19], as is roughly the case when fast H_3^+ projectiles collide with noble gas targets ranging from He to Xe [7]. In a FCM description this process corresponds to a free electron colliding with a noble gas target and receiving a large enough momentum transfer, either from the target nucleus or the target electrons. A similar process occurs when fast electrons ionize noble gas targets, with cross sections proportional to target sizes alternatively given by $\langle r_{nl}^2 \rangle$ or $(\langle r_{nl} \rangle)^2$, where n and l are the quantum numbers of the ejected electron [20] (for the present velocity range this means the valence target electron). Collisional destruction of fast molecules and atoms may then present a similar target-size dependence and in order to investigate this possibility the ratios of the destruction cross sections in Ar-He, Ne-He, and Ar-Ne are respectively presented in Tables VI, VII, and VIII for the

TABLE III. Normalized destruction cross sections S for a He target and H_2, H_2^+, and H_3^+ projectiles, divided by S_H.

Velocity (a.u.)	$S_{projectile}/S_H$		
	H_2^+	H_2	H_3^+
3.0	0.82±0.16	0.71±0.13	0.78±0.16
4.0	1.12±0.19	0.88±0.12	1.01±0.17
5.0	1.34±0.20	0.99±0.12	1.19±0.19
6.0	1.50±0.21	1.04±0.12	1.32±0.21
7.0	1.61±0.26	1.09±0.12	1.40±0.22

TABLE IV. Normalized destruction cross sections S for a Ne target and H_2, H_2^+, and H_3^+ projectiles, divided by S_H.

Velocity (a.u.)	$S_{projectile}/S_H$		
	H_2^+	H_2	H_3^+
3.0	0.94±0.10	0.71±0.18	0.86±0.15
4.0	0.95±0.09	0.74±0.18	0.86±0.15
5.0	0.96±0.10	0.76±0.18	0.86±0.14
6.0	0.97±0.10	0.79±0.20	0.86±0.14
7.0	0.98±0.10	0.81±0.21	0.86±0.14

TABLE V. Normalized destruction cross sections S for an Ar target and H_2, H_2^+, and H_3^+ projectiles, divided by S_H.

Velocity (a.u.)	$S_{projectile}/S_H$		
	H_2^+	H_2	H_3^+
3.0	1.0±0.12	0.87±0.13	0.94±0.16
4.0	1.0±0.12	0.87±0.12	0.94±0.16
5.0	1.0±0.12	0.87±0.13	0.90±0.15
6.0	1.0±0.12	0.87±0.13	0.83±0.14
7.0	1.0±0.12	0.87±0.14	0.81±0.14

TABLE VI. Ratio of the Ar and He target destruction cross sections for the projectiles H_2, H_2^+, H_3^+, and H.

Velocity (a.u.)	$\sigma_D(Ar)/\sigma_D(He)$			
	H_2	H_2^+	H_3^+	H
3.0	5.9±1.1	6.1±1.0	6.8±1.4	4.8±0.7
4.0	7.2±1.2	6.7±1.1	7.6±1.6	7.2±0.8
5.0	8.3±1.4	7.6±1.3	8.6±1.8	9.5±0.9
6.0	9.4±1.6	7.6±1.3	9.2±1.9	11.0±1.0
7.0	10.3±1.8	8.0±1.4	9.7±2.0	13.0±1.2

TABLE VII. Ratio of the Ne and He target destruction cross sections for the projectiles H_2, H_2^+, H_3^+, and H.

Velocity (a.u.)	$\sigma_D(Ne)/\sigma_D(He)$			
	H_2	H_2^+	H_3^+	H
3.0	2.8±0.8	3.1±0.5	3.7±0.8	2.8±0.4
4.0	3.3±0.8	3.3±0.6	3.8±0.8	3.9±0.4
5.0	3.6±0.9	3.4±0.6	4.0±0.8	4.7±0.4
6.0	4.0±1.0	3.5±0.6	4.1±0.9	5.4±0.5
7.0	4.3±1.2	3.6±0.6	4.1±0.9	5.8±0.5

TABLE VIII. Ratio of the Ar and Ne target destruction cross sections for the projectiles H_2, H_2^+, H_3^+, and H.

Velocity (a.u.)	$\sigma_D(Ar)/\sigma_D(Ne)$			
	H_2	H_2^+	H_3^+	H
3.0	2.1±0.6	1.9±0.2	1.8±0.4	1.7±0.2
4.0	2.2±0.6	1.9±0.2	2.0±0.4	1.9±0.2
5.0	2.3±0.6	2.0±0.2	2.1±0.4	2.0±0.2
6.0	2.3±0.6	2.0±0.2	2.2±0.5	2.1±0.2
7.0	2.4±0.7	2.1±0.3	2.3±0.5	2.2±0.2

different projectiles H_2, H_2^+, H_3^+, and H. As expected, the cross sections vary very roughly with the target size (the respective $(\langle r_{nl} \rangle)^2$ values for He, Ne, and Ar are 0.86, 0.94, and 2.75 a.u. [21]). Besides that there are velocity dependences which, for a given pair of targets, behave similarly for different projectiles, with a stronger monotonic increase in Table VI and a weaker one in Table VIII. This similarity may indicate that the size of the compound system formed during the collision is the relevant one and, as the molecular projectiles have similar sizes (the average internuclear distances in H_2, H_2^+, and in H_3^+ are, respectively, 0.8, 1.1, and 0.9 Å), the compound molecular noble gas systems also present similar sizes.

These results motivated us to compare the molecular ion destruction with the corresponding processes in the atomic systems H and H^-. It seems that the model works very well for H atoms colliding with He, Ne, and Ar, as shown in Tables III, IV, and V. Difficulties arise, however, when we try to make a simple description of H^- as a two-electron system with an electron affinity of 0.755 eV. The experimental results of Ref. [17] have shown a very strong electron-electron correlation underlying the mechanisms governing the electron loss from H^-. The semiempirical treatment of Ref. [15] for H and H^- electron loss also points in that direction, with the projectile orbital electron velocities that fit the model differing only by a factor of 2. In fact, when we tentatively calculate the normalized cross sections S_{H^-} for the three targets, considering 0.755 as the binding energy of the ejected electron, we get values an order of magnitude lower than the ones for H, H_2, H_2^+, and H_3^+. This indicates that the strong H^- electron correlation prevents the use of this simple independent-particle model for the H^- projectile.

IV. CONCLUSIONS

Total destruction cross sections for fast H_2 molecules (velocities in the 3.0–7.0 a.u. range) incident on He, Ne, and Ar targets and for H_2^+ colliding with Ne (3.0–7.0 a.u.) and with He and Ar (3.0 a.u.) have been measured. The simple model proposed by Salpeter a long time ago [13] is able to reproduce well our present H_2 and H_2^+ results, and also our previous H_2^+ and H_3^+ results. In all three cases, the average internuclear distances are almost the same, and this, together with the small correlation of the H_2 and the H_3^+ electrons and the possibility of defining a dissociation energy, leads to a normalization procedure for the cross sections which then becomes projectile independent. This procedure, consisting in defining a normalized cross section $\sigma I/n$, also gives a good agreement for the smaller H atomic projectiles but does not work for H^- projectiles, due to the strong correlation between its two electrons. Concerning the main H_2 destruction channel, the experimental results strongly point to ionization and not to the direct excitation of the $b\,^3\Sigma_u^+$ dissociative state. The target dependence of the destruction cross sections, as given by cross section ratios for different targets, is remarkably identical for all three molecular projectiles. This fact may

be, together with the success of the simple normalization procedure here employed, a guide for more sophisticated models taking into account accurately the projectile and target form factors.

On the experimental side, in the future the destruction of HeH^+ ions will be studied, for the same target gases and velocity range. These molecular ions are important due to their similarity with the three other molecules already studied by our group, being diatomic like $H_2{}^+$ and H_2 and possessing two electrons like $H_3{}^+$ and H_2, thus leading to the question whether they will behave similarly.

ACKNOWLEDGMENTS

This work was partially supported by CNPq and FINEP.

[1] D. Nir, A. Weinberg, A. Mann, M. Meron, and S. Gordon, Phys. Rev. A **18**, 1399 (1978); D. Nir, E. Navon, A. Ginzburg, and A. Mann, *ibid.* **28**, 2796 (1983).
[2] K.H. Berkner, T.J. Morgan, R.V. Pyle, and J.W. Stearns, Phys. Rev. A **8**, 2870 (1973).
[3] I.D. Williams, J. Geddes, and H.B. Gilbody, J. Phys. B **17**, 811 (1984).
[4] M.J. Gaillard, A.G. de Pinho, J.C. Poizat, J. Remillieux, and R. Saoudi, Phys. Rev. A **28**, 1267 (1983).
[5] N.V. de Castro Faria, I. Borges, Jr., L.F.S. Coelho, and Ginette Jalbert, Braz. J. Phys. **23**, 237 (1993).
[6] G.W. McClure, Phys. Rev. **130**, 1852 (1963); J.F. Williams and D.N.F. Dunbar, *ibid.* **149**, 62 (1966).
[7] Wania Wolff, L.F.S. Coelho, H.E. Wolf, and N.V. de Castro Faria, Phys. Rev. A **45**, 2978 (1992).
[8] N.V. de Castro Faria, Wania Wolff, L.F.S. Coelho, and H.E. Wolf, Phys. Rev. A **45**, 2957 (1992).
[9] Ginette Jalbert, L.F.S. Coelho, and N.V. de Castro Faria, Phys. Rev. A **46**, 3840 (1992).
[10] Ginette Jalbert, L.F.S. Coelho, and N.V. de Castro Faria, Phys. Rev. A **47**, 4768 (1993).
[11] N.V. de Castro Faria, M.J. Gaillard, J.C. Poizat, and J. Remillieux, Nucl. Instrum. Methods Phys. Res. Sect. B **43**, 1 (1989).
[12] D. Nir, A. Mann, and J. Kantor, Phys. Rev. A **18**, 156 (1978); S. Abraham, D. Nir, and B. Rosner, *ibid.* **29**, 3122 (1984).
[13] E.E. Salpeter, Proc. Phys. Soc. London Sect. A **63**, 1295 (1950).
[14] H. Tawara, Y. Itikawa, H. Nishimura, and M. Yoshino, J. Phys. Chem. Ref. Data **19**, 617 (1990).
[15] M. Meron and B.M. Johnson, Phys. Rev. A **41**, 1365 (1990).
[16] N. Bohr, D. K. Dan. Vidensk. Selsk. Mat.-Fys. Medd. **XVIII**, 8 (1948).
[17] D.P. Almeida, N.V. de Castro Faria, F.L. Freire, Jr., E.C. Montenegro, and A. G. de Pinho, Phys. Rev. A **36**, 16 (1987).
[18] T.E. Sharp, At. Data **2**, 119 (1971).
[19] J.F. Williams and D.N.F. Dunbar, Phys. Rev. **149**, 62 (1966).
[20] J.W. Otvos and D.P. Stevenson, J. Am. Chem. Soc. **78**, 546 (1956); P. Tiwari, D.K. Rai, and M.L. Rustgi, J. Chem. Phys. **50**, 3040 (1969).
[21] C.F. Fischer, *The Hartree-Fock Method for Atoms* (Wiley, New York, 1977).